energies

MDPI

Article

Patents Analysis of Thermal Bridges in Slab Fronts and Their Effect on Energy Demand

David Bienvenido-Huertas [1,*], Juan Antonio Fernández Quiñones [1], Juan Moyano [1] and Carlos E. Rodríguez-Jiménez [2]

[1] Department of Graphical Expression and Building Engineering, University of Seville, 41012 Seville, Spain; juanan.fdezq@gmail.com (J.A.F.Q.); jmoyano@us.es (J.M.)
[2] Department of Building Construction II, University of Seville, 41012 Seville, Spain; ceugenio@us.es
* Correspondence: jbienvenido@us.es; Tel.: +34-954-556-626

Received: 14 July 2018; Accepted: 20 August 2018; Published: 24 August 2018

Abstract: Nowadays, the building sector is one of the main sources emitting pollutant gases to the atmosphere due to its deficient energy behaviour. Among the elements of the envelope, the thermal bridges are where the heat losses and gains mainly occur, depending on the season of the year. To reduce the effect of the thermal bridges, there are different patented technologies which give provide solutions. In this paper, the thermal behaviour of five patented slab front (slab-façade) thermal bridges are analysed in a case study located in the south of Spain. Moreover, the influence of the thermal bridge on the energy demand from the building analysed was evaluated, both in the current scenario and future ones (2020, 2050 and 2080). The results reveal that the use of the patents in slab fronts can mean reductions by up to 95.74% in the linear thermal transmittance. Likewise, due to the improvement of the thermal bridge of slab fronts by using the patented designs which offered the best features, a savings in the global energy demand for heating higher than 18% as well as a savings in the global energy demand for cooling higher than 2.80% could be achieved in all the time scenarios considered.

Keywords: patents; thermal bridges; slab fronts; linear thermal transmittance; energy demand

1. Introduction

The energy consumption of buildings is causing serious consequences for the environment. In 2014, the building sector was responsible for 24.79% of the energy consumption in the European Union [1]. Furthermore, this sector tends to produce a higher energy consumption per year (it has been causing an annual increase of 1% since 1990) [2]. In order to reduce the energy consumption from the existing building stock, the European Union has developed the roadmap for a low-carbon economy [3]. The objective pursued by this research is to reduce the pollutant gas emissions by 80% by 2050. For this purpose, the building sector should reduce the pollutant gas emissions by 90% by cutting down its energy consumption. Thus, one of the main challenges of today´s society is the energy modernization of the existing building stock as well as the design of new efficient buildings, mainly to guarantee an adequate behaviour of the buildings in future climate scenarios [4,5].

Among the different elements which compose the building, the envelope is among those which has a more significant effect on energy behaviour [6–8]. Highly efficient thermophysical properties for the envelope allow one to significantly reduce the energy demand of buildings [9]. This envelope is normally constituted by a series of layers of different thicknesses and thermal conductivities which determine its thermal transmittance. However, there are areas of the envelope where the junction of different elements causes a thermal bridge. Thermal bridge is understood as the part of the envelope which shows variations in the thermal resistance due to factors such as the presence of materials with a

high thermal conductivity and geometrical variations, as occurs in the junctions between walls, floors, ceilings or windows [10].

These thermal bridges are responsible for causing heat losses in winter and heat gains in summer [11,12]. In this sense, thermal bridges can lead to variations up to 30% in the heating demand, even in those buildings with envelopes having high insulation thickness [13]. This occurs because the thermal bridge can increase the thermal transmittance value of a wall up to 35% [14]. Thus, due to the low thermal resistance and the energy losses associated, the analysis of thermal bridges will influence significantly the energy demand of the building as well as the determination of the energy conservation measures (ECMs) to be carried out [15,16]. In addition, thermal bridges are responsible for certain pathologies which can appear in buildings, such as the appearance of areas with mould and condensation due to the reduction of the internal surface temperature [17], as well as the material degradation because of these damages [18].

The detection and quantification of thermal bridges are among those most important activities to be carried out in energy audits. The use of tests such as the infrared thermography or the blower door allow one to find certain thermal bridges [19]. Regarding their quantification, the ISO standard 10211 [10] establishes a calculation procedure for two-dimensional and three-dimensional evaluations yielding adequate results [20]. In spite of the existence of software which calculates the linear thermal transmittance with a high accuracy (for example, THERM), the characterization of thermal bridges constitutes one of the main study gaps in the last years: (i) Asdrubali et al. [21,22], Bianchi et al. [23], Garrido et al. [24], and O'Grady et al. [25,26] presented different methodologies to detect automatically and quantify thermal bridges through thermographies; (ii) Zalewski et al. [27] developed a methodology of characterization of thermal bridges by means of three-dimensional modelling, and compared the results with measurements using temperature probes and thermographies; (iii) Tadeu et al. [28] proposed a special methodology of quantification of thermal bridges through a boundary element model; and (iv) Dilmac et al. [29] suggested a particular method of two-dimensional evaluation of the thermal bridge slab, beam and wall.

Moreover, the quantification of thermal bridges in real case studies and their influence on the energy behaviour of buildings constitutes one of the main lines of research in the last years. In the scientific literature, there are several studies conducted on different thermal bridge typologies. Theodosiou and Papadopoulos [30] studied the impact of the thermal bridges of Greece´s representative wall construction configurations on the energy demand, and determined that including thermal bridges in the calculation methodology of the energy demand is fundamental to determine it accurately. In a later study, Theodosiou et al. [31] studied thermal bridges in metal cladding systems, determining how the building design influences heat losses. Ramalho de Freitas and Grala da Cunha [32] evaluated the impact of the thermal bridges of reinforced concrete structures on the energy behaviour of a building in Brazil, proving that the energy demand can vary by up to 20%. In a study by Ge et al. [33], the influence of thermal bridges caused through the balconies was analysed in residential building in Canada. Results showed an influence between 5 and 13% on the heating energy demand, and of 1% in cooling energy demand. Zedan et al. [34] studied the effect of thermal bridges generated by mortar joints, capable of causing even an increase of 15% in the internal loads of the building. Song et al. [35] studied thermal bridges in metal panel curtain wall systems, proposing different options that achieved a 68% reduction in the heat loss by 68%. Ascione et al. [20] studied thermal bridges of flat heterogeneous roofs in a typical office building located in four different climate regions in Italy. These thermal bridges were obtained by means of simplified 1-D models and 2-D models. The use of the 2-D model allowed the authors to determine a more accurate estimation of the energy behaviour of the building. Evola et al. [36] carried out another study in Italy where the effect of thermal bridges on two different semi-detached houses located in a mild Mediterranean climate was studied, determining that the improvement of the thermal bridges led to a decrease of the heating load by 25%, and of the cooling load by 8.5%.

Recent studies [37–39] have analysed thermal bridges generated by lightweight steel-framed (LSF) walls due to the high thermal conductivity of the steel studs. Santos et al. [37] studied the importance of the flaking heat loss in LSF walls, determining that the thermal transmittance can vary from −22% for the external surface to +50% for the internal surface, and the metal fixation elements are one of the most important elements. The use of mitigation techniques, such as thermal break strips and slotted steel profiles, could lead to reduce the thermal transmittance by 8.3% [38]. In a later study [39], the authors evaluated the effectiveness of the position of thermal insulation in LSF walls by analysing three different types of construction (cold, warm, and hybrid construction). The results determined that the warm construction (insulation from the exterior) is the typology of LSF walls less affected by the thermal bridge.

Levinskyte, Banionis and Geleziunas [40] analysed the importance of thermal bridges in highly efficient buildings in Lithuania, and the heat losses between the walls and the slab were among the most important joints. The junction between the slabs and the façades are one of the most complicated junctions in order to decrease the thermal bridge, since these junctions are consolidated building elements that should be studied during the design phase to be able to cause efficient constructive solutions. To do this, there are nowadays different patents proposing construction solutions to reduce the heat losses of thermal bridges in slab fronts. However, there are no studies where the efficiency of such patents is analysed.

The previous review reveals the importance of decreasing scientifically the heat losses through thermal bridges due to their influence on the energy behaviour of the building. However, there are no studies where the existing patents to reduce heat losses or gains through thermal bridges have been profoundy analysed. Thus, the objective of this work was to analyse the thermal behaviour of some existing patents describing construction solutions for slab fronts, focusing on these junctions due to their significant influence on heat losses through the façade [40]. For this purpose, five different solutions were chosen and applied on a real case study. The heat transfer for the five patented designs was analysed by two-dimensional calculation using the THERM software, and both the value of linear thermal transmittance and the temperature factor for the interior surface were obtained, thus identifying the patent with the best behaviour. Likewise, the effect that the best patent had on the energy behaviour of a building was studied, both in current and future scenarios with the effect of the climate change (2020, 2050, 2080). To do this, energy simulations were carried out using the Design Builder software (which includes the Energy Plus calculation engine) by introducing the value of linear thermal transmittance obtained by the patent with the best thermal behaviour.

2. Patents Studied

To analyse the thermal bridges, five patents of constructive solutions of thermal bridges different in design, materials and work execution were chosen. The patents considered are listed below and ordered by year of publication (see Figure 1):

- Patent 1, by Société Générale d'Entreprises Construction [41] and published in 1984.
- Patent 2, by Egger [42] and published in 1985.
- Patent 3, by François [43] and published in 2003.
- Patent 4, by López Muñoz [44] and published in 2012.
- Patent 5, by Ortega López et al. [45] and published in 2015.

Patent 1 consists of the creation of a formwork lost for the slab by creating a box made by metal panels where an insulating material is placed. Unlike other patents described below, the external masonry leaf does not present discontinuities along the surface, so the thickness of the insulating material is limited by this design condition.

Patent 2 proposes a constructive solution similar to that from Patent 1, but metal panels are not used in this case. This patent consists of a thermal insulation panel joined to the slab by a metal bar frame.

Patent 3 consists of introducing an insulating material membrane of multiple reflector type in both all the slab front and inferior and superior overlapping, as well as a plaster panel.

Patent 4 is similar to Patent 3. The design consists of putting a covering membrane in both slab front and some part of its inferior and superior sides. This covering membrane is constituted by two layers of polyethylene and an aluminium membrane.

Finally, the last patent studied (Patent 5) is an evolution of Patent 2. This construction solution consists of a metal structure of bars with thermal insulation fixed to the perimeter beams before concreting, using an insulating material: extruded polystyrene (XPS) or polyurethane (PUR), with a thickness between 20 and 60 mm.

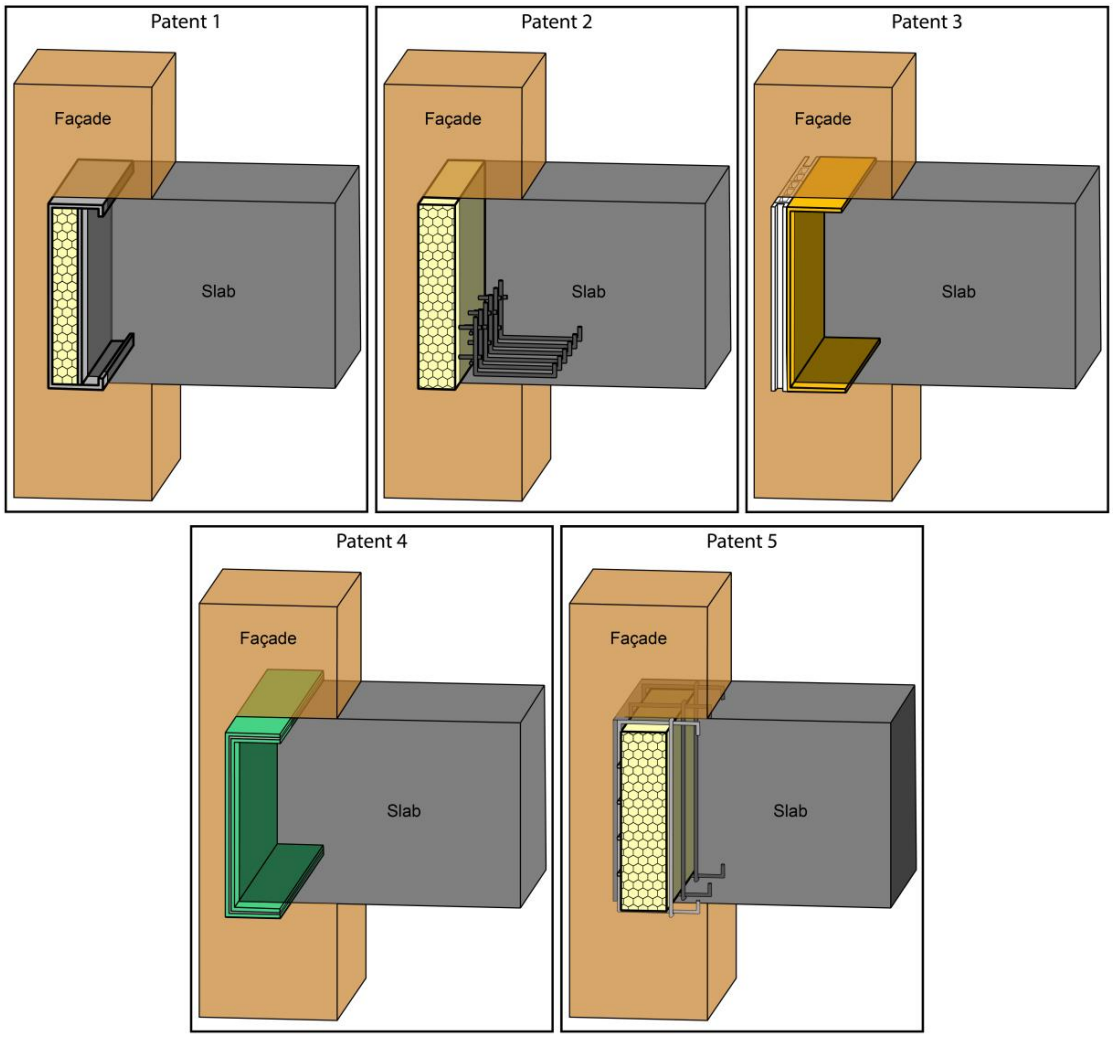

Figure 1. Detail of the patents analysed.

3. Case Study

3.1. Analysed Building

The building chosen is a typical building from the south of Spain, built in 2008. The building has a height of three floors over the building line and the bulkhead. There are six dwellings: two on the ground floor, two on the first floor, and two on the second floor (see Figure 2). The northern and southern side walls have no windows and are the dividing walls with respect to the adjacent buildings. The main façade faces West. There are also two courtyards: an interior courtyard allowing the opening

of windows in the most internal areas, and an exterior courtyard in the eastern façade, which is only available for the dwellings on the ground floor.

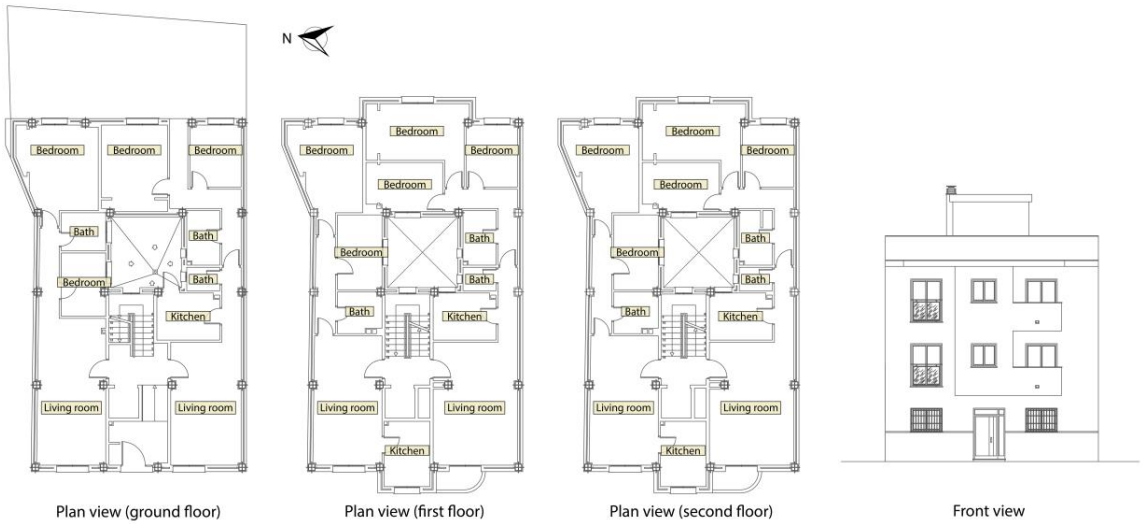

Figure 2. Graphical representation of floors and elevations of the building analysed.

The building was chosen because it was a typical building of the area and had thermal bridge problems (see Figure 3). Moreover, technical documentation was available to characterize it correctly. Thus, the composition of the façade was determined following the methodology established by Ficco et al. [46] of using reliable technical documentation. Table 1 indicates the relationship of layers that constitute the façade as well as their thermophysical properties.

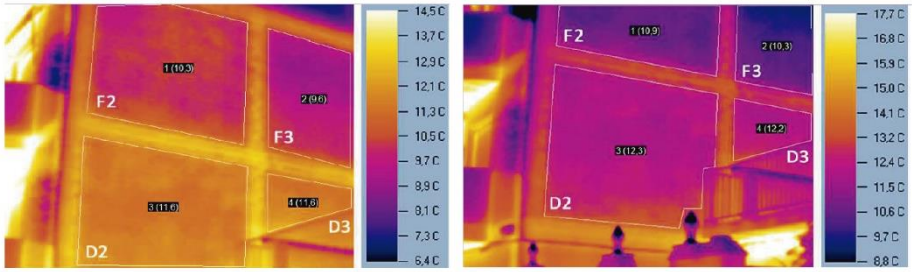

Figure 3. Thermographies of the analysed building carried out according to the ISO standard 6781 [47].

Table 1. Layer thickness and thermophysical properties of the building façade.

#	Layers	*S* (mm)	*λ* (W/(mK))	*R* ((m^{2}K)/W) [a]	eSketch
1	Cement mortar	10	0.70	-	
2	Perforated brick	110	0.59	-	
3	Cement mortar	10	1.30	-	
4	PUR insulation	20	0.03	-	
5	Air gap	40	-	0.18	
6	Hollow brick	50	0.44	-	
7	Gypsum plaster	10	0.40	-	
$R_{s,in}$ = 0.13 (m^{2}K)/W [a]		$R_{s,out}$ = 0.04 (m^{2}K)/W [a]		-	

[a] Thermal resistance obtained from ISO 6946 [48].

3.2. Climate Zone

The building is situated in Seville, in the south of Spain. The city is located in the Csa climate zone [49], characterized by dry and hot summers as well as mild winters, where the maximum temperature during the heating season can reach 36 °C, and the average temperature in winter is 10 °C (see Table 2).

Table 2. Average temperatures in EnergyPlus Weather (EPW) file from the city of Seville.

Month	Average Temperature (°C)	Average Maximum Temperature (°C)	Average Minimum Temperature (°C)
January	10.35	15.79	5.57
February	11.74	17.96	6.92
March	15.11	22.23	8.94
April	16.07	23.15	9.64
May	19.78	26.77	12.56
June	24.09	31.84	16.65
July	27.42	36.43	19.24
August	26.52	34.99	18.76
September	24.47	32.60	16.95
October	19.55	25.63	14.34
November	13.72	19.87	9.18
December	11.53	17.06	7.30

3.3. Virtual Modelling

As mentioned previously, the modelling of the thermal bridges was carried out by using the THERM software. Six configurations were modelled as follows: (i) construction section that the building currently has; (ii) construction section with Patent 1; (iii) construction section with Patent 2; (iv) construction section with Patent 3; (v) construction section with Patent 4; and (vi) construction section with Patent 5. The thermophysical properties indicated in the project were used as thermophysical properties of the materials of the constructive solution. Internal and external conditions were defined from the long-term monitoring of the building (see Figure 4). Measurements were performed in the living room on the first floor. Based on the monitoring, it was determined that the maximum temperature differences obtained were of 10 °C. For this reason, an indoor temperature of 20 °C and an outdoor temperature of 10 °C were defined in the simulations made by THERM.

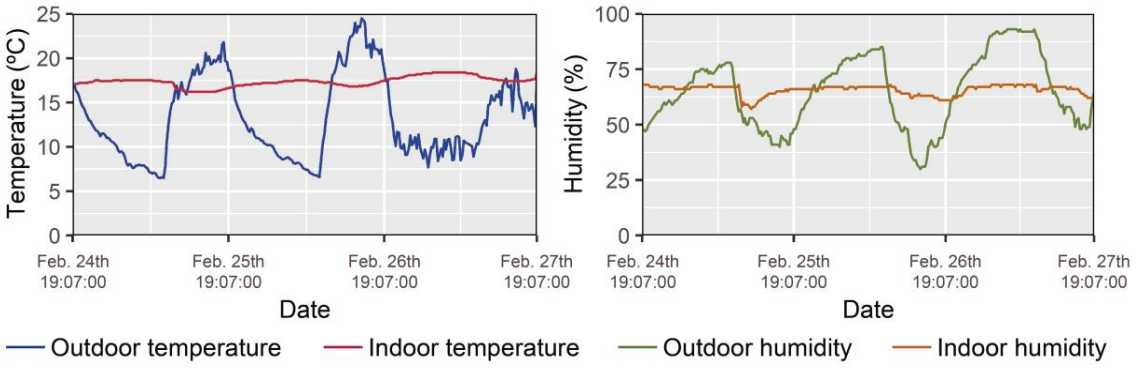

Figure 4. Part of the monitored time series of indoor and outdoor temperature and humidity of the building.

As the THERM software has been validated according to the standard EN ISO 10211 in several studies [39,50,51], the aim of verifying the models developed using THERM was the determination of the possible differences in the inputs from the model as well as the thermophysical properties of

the materials. To do this, two-dimensional simulations of the same thermal bridges were carried out by the HTFlux software, using the same boundary conditions and material properties (see Figure 5), and the average values of thermal transmittance obtained were compared.

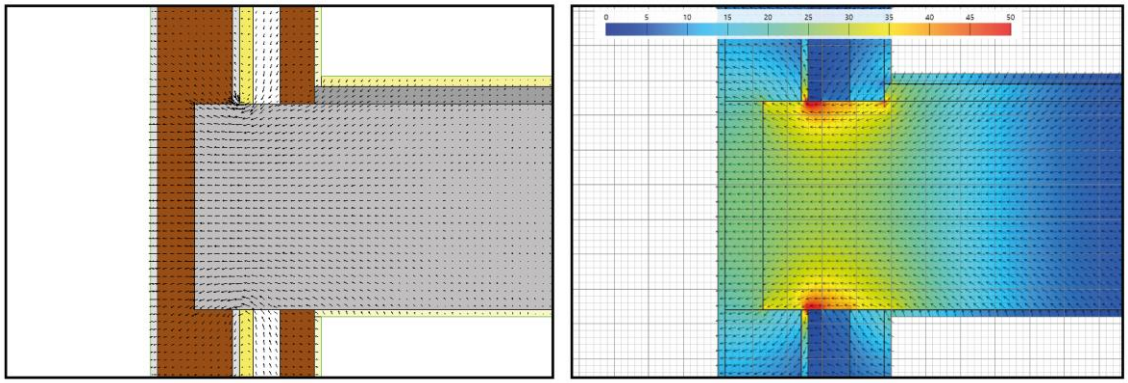

Figure 5. (**a**) Modelling of the thermal bridge of the slab front carried out using THERM and (**b**) Modelling of verification carried out using HTFlux.

The modelling of the building was performed by using the EPW file from the Design Builder software for the city of Seville. To obtain the climate scenarios for the years 2020, 2050 and 2080, a morphing process was carried out [52–54]. The CCWorldWeatherGen software was used to perform the morphing process [54]. This morphing process [52–54] uses the meteorological data of the EPW files with United Kingdom Met Office Hadley Centre general circulation model (GCM) predictions for the A2 scenario (intermediate-high) of greenhouse gas emissions effects [55], generating time series for 2020, 2050, and 2080. For this, the morphing process uses three different algorithms depending on the variable to be modified. These algorithms are widely described by Belcher et al. [52].

There are studies where the importance of using the morphing process to obtain future scenarios is shown [4,5,52,54], since these scenarios are generated by using a current meteorological dataset, although extraordinary natural phenomena associated with the climate change (hurricanes or storms) are not considered [4].

Thus, when the morphing process was finished, three EPW files from the city of Seville were generated with the modified climate variables under A2 emissions scenario for the years 2020, 2050, and 2080.

By using these four climate scenarios (current, 2020, 2050, and 2080), eight different cases of energy simulation (see Table 3) could be established on the model of the building carried out using Design Builder (see Figure 6).

Table 3. Configuration of the energy simulation cases analysed.

Cases	EPW File of Seville	Type of Thermal Bridge
Case 1	Current	Not patented
Case 2	2020	
Case 3	2050	
Case 4	2080	
Case 5	Current	With the thermal bridge patent that the best linear thermal transmittance obtained
Case 6	2020	
Case 7	2050	
Case 8	2080	

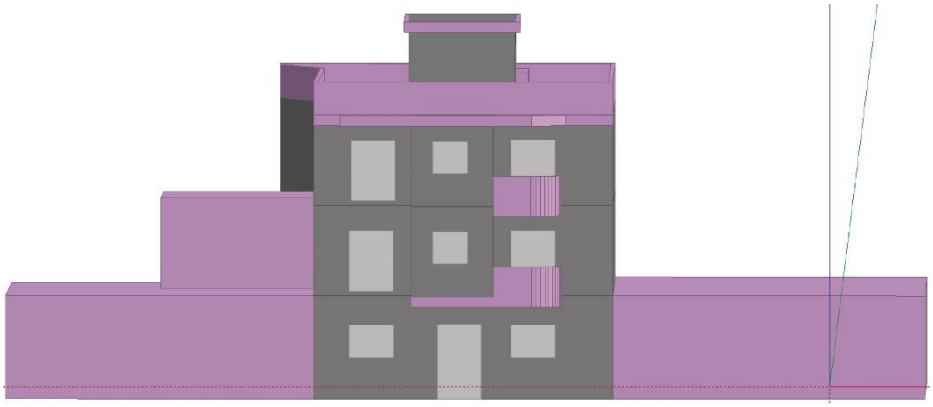

Figure 6. Modelling of the building performed using Design Builder.

In all simulated cases, the rest of the building model parameters, such as use profiles or HVAC systems, were not modified. In this sense, it is important to highlight the configured parameters regarding the use profiles, the efficiency of cooling and heating systems, air turnovers, and internal heat gains.

The use profile was defined with a percentage between 50% and 100%, except during working hours (from 7:00 a.m. to 3:00 p.m.) in which a use of 10% was established. Due to the climate conditions of the area, heating and cooling systems were considered to be used in atypical months (e.g., using cooling in cold months if the set point temperatures are exceeded). For the cooling, the set point temperature was of 25 °C and the setback temperature of 27 °C, whereas for the heating, the set point temperature was of 20 °C and the setback temperature of 17 °C. The heating system had a Coefficient of Performance (CoP) of 0.85, and the cooling system had a CoP of 1.80.

With respect to the ventilation rate, the use profiles used where those established by the technical standard in Spain [56]. The number of air changes per hour for all the year was 0.63 ac/h by means of mechanical ventilation. The only exception corresponded to summer, between 1:00 and 8:00 a.m., since the technical standard established that ventilation should be natural (due to the opening of the windows) and the rate to be used should be of 4.00 ac/h in that period.

For the internal heat gains, the use profile of lightning systems was established, as well as the equipment in the house established by the technical standard in Spain, with a density of maximum power of 4.4 W/m^2. The metabolic rate of the occupants was defined according to what it is indicated in Table 5 of chapter 8 in the ASHRAE Handbook of Fundamentals [57].

4. Results and Discussion

4.1. Patent Analysis of Thermal Bridges of Slab Fronts

The simulation of the patents using THERM allowed us to prove the improvements produced by the different constructive solutions. Firstly, the representation of the models generated by THERM was determined. To do this, the existing differences between the thermal transmittance values obtained by both software for each construction solution were analysed. As can be appreciated in Table 4, the thermal transmittance results obtained for each construction solution presented deviations of less than 4.5%, and these differences were due to the possibility of configuration of the materials that both software allowed. Thus, as big differences between both simulations were not obtained, the models of the construction solutions carried out using THERM were representative.

Table 4. Results of thermal transmittance obtained for each constructive solution analysed using THERM and HTFlux software, and the existing difference.

Models	U_{THERM} (W/(m^2·K))	U_{HTFlux} (W/(m^2·K))	Percentage Deviation (%)
Without patent	1.101	1.075	2.37
Patent 1	1.044	0.999	4.33
Patent 2	0.876	0.877	−0.16
Patent 3	1.002	1.019	−1.66
Patent 4	1.110	1.088	1.96
Patent 5	0.836	0.838	−0.24

After validating the representation of the models generated by THERM, linear thermal transmittance results of the different patents were obtained. To obtain the linear thermal transmittance (Equation (1)), the software provides the factor of thermal coupling (Equation (2)), which is fundamental to calculate the linear thermal transmittance:

$$\psi = L^{2D} - \sum_{j=1}^{n} l_j U_j \quad (1)$$

$$L^{2D} = \frac{q}{T_{in} - T_{out}} \quad (2)$$

where ψ is the linear thermal transmittance (W/(m·K)); L^{2D} is the factor of two-dimensional coupling (W/(m·K)); l_j is the length of the two-dimensional geometric model (m); U_j is the thermal transmittance of the one-dimensional component j (W/(m^2·K)); T_{in} is the indoor air temperature (K); and T_{out} is the outdoor air temperature (K).

In Figure 7, the values of linear thermal transmittance obtained for each simulated building configuration are represented. As can be proved, the results showed how the linear thermal transmittance decreased using almost all the patents considered. In this sense, Patent 5 was the one which obtained the lowest linear thermal transmittance, a decrease by 95.74% with respect to the construction solution without slab front. The other solutions obtained lower improvements than Patent 5: Patent 1 achieved a decrease by 20.06% with respect to the case study without patent; Patent 2 achieved a decrease by 80.40%, being the patent with the second best results; Patent 3 obtained a decrease by 36.32%. Only Patent 4 obtained a higher linear thermal transmittance than the case study without patent, with an increase by 3.50%. This is because this patent did not use an insulating material, since it only included polyethylene (with a thermal conductivity of 0.33 W/(m·K)) and aluminium (with a thermal conductivity of 230 W/(m·K)). Thus, the combination of both materials made the linear thermal transmittance obtainedhigher than that from the study assumption without modification.

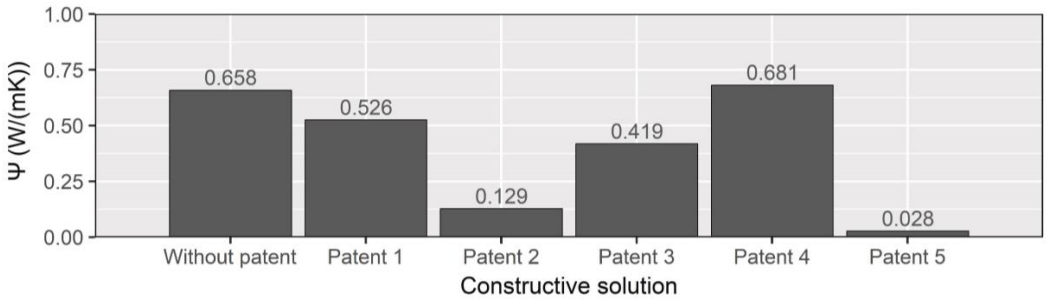

Figure 7. Results of linear thermal transmittance obtained for each constructive solution analysed.

Furthermore, the surface temperature factor ($f_{R,si}$) (Equation (3)) was determined by the simulation carried out by THERM to analyse the possibility of condensation generated inside the

building. For this purpose, the internal surface temperature ($T_{s,in}$) of each construction solution was measured in the point with the lowest temperature thanks to the isotherm profiles generated in each simulation (see Figure 8).

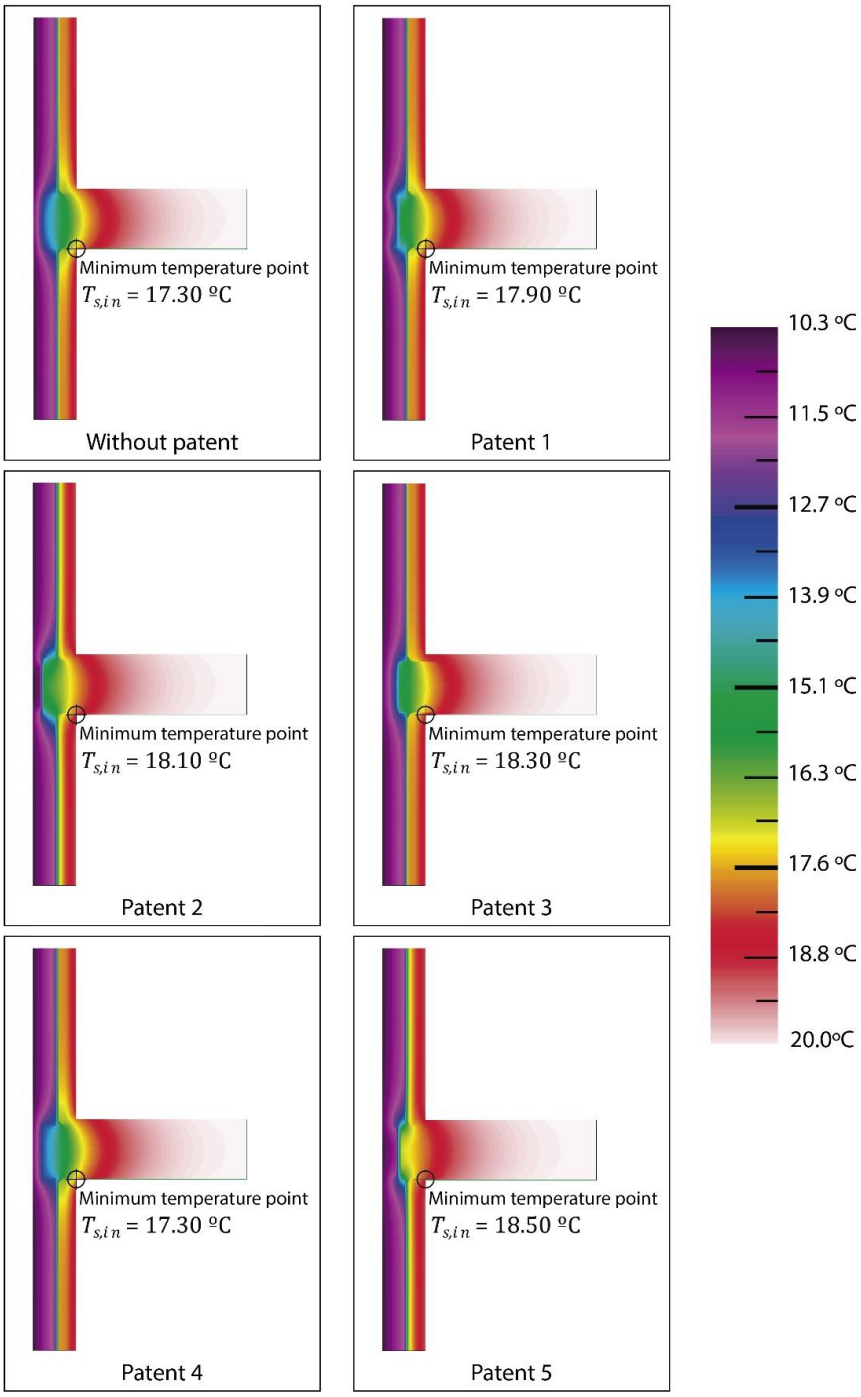

Figure 8. Isotherm profiles for each constructive solution analysed.

Figure 8 shows that the point with the lowest temperature (the joint between the inferior side of the slab and the façade) was the same for all the building configurations considered. The results reflected slight variations in the factor $f_{R,si}$ for the different construction solutions. The construction solution without patent obtained a temperature factor of 0.865, which exceeded the minimum value required by the technical standard in Spain for the climate region of Seville (0.52) [56]. The remaining patents

obtained the same or higher values of factor $f_{R,si}$, so all the analysed building configurations did not cause condensations (see Figure 9). The patent with the best factor $f_{R,si}$ was Patent 5 with a value of 0.925, followed by Patents 2 and 3 with factors of 0.905 and 0.915, respectively. As similarly occurred for the linear thermal transmittance, Patent 4 obtained the same factor $f_{R,si}$ as for the constructive solution without patent, so its design did not influence the decrease of condensation risk. Therefore, among the different patents analysed, Patent 5 had best features in the case study analysed, since this patent achieved the lowest linear thermal transmittance as well as the best temperature factor for the interior surface:

$$f_{R,si} = \frac{T_{s,in} - T_{out}}{T_{in} - T_{out}} \quad (3)$$

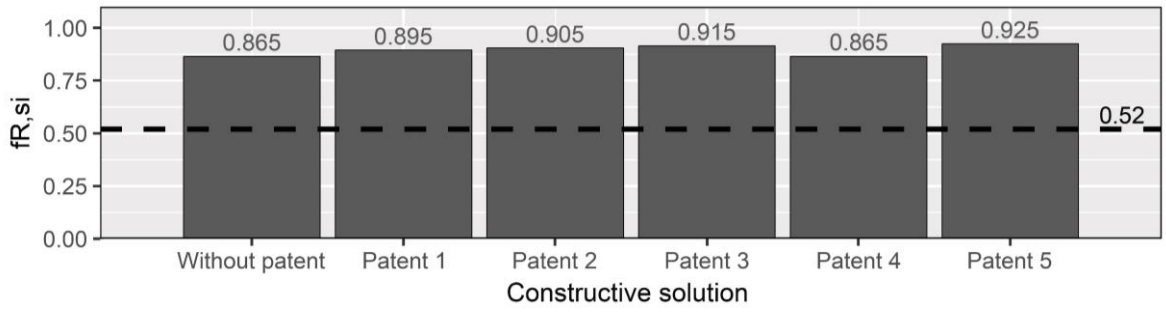

Figure 9. Internal surface temperature factor in all the assumptions. The minimum factor $f_{R,si}$ required by the technical standard in Spain is represented by black line.

4.2. Influence of Thermal Bridge of the Slab Front on Energy Demand

After determining the patent with best results in the building analysed, its influence on the energy demand was studied. For this purpose, and as mentioned in Section 3.3, eight different simulations were carried out: four corresponding to the building without patent, and four to the building with the best patent, aiming at assessing the effects of climate change on the energy demand of the building. In Figure 10, the values of heating and cooling demand obtained for each simulation (building with and without patent) are represented. Regarding the analysis generated by using the EPW files for the different time scenarios (current, 2020, 2015, and 2018), the increase of external temperatures in the different time scenarios caused the decrease of the heating energy demand, reaching decreases higher than 1000 kWh, and even removing the heating demand in future scenarios (June and September of 2050 and 2080) with respect to the current scenario. On the other hand, the increase of external temperatures led to increasing the cooling energy demand in the different simulations, with an increase by 82.03% in July, and by 74.54% in August of 2080 with respect to the values obtained in the current scenario.

The use of the building patent allowed to reduce the energy demand of the building in all the scenarios considered (see Figure 10). In Tables 5–8, the values obtained of energy demand for the different periods considered as well as the percentage deviations are indicated. As can be appreciated, the effect generated by the building patent on the monthly energy demand depends on the type of demand: the heating energy demand was more influenced by the effect of the thermal bridge than the cooling energy demand. In this sense, the energy demand for heating in the current scenario could be reduced up to 15.44% during the months characterized by lower temperatures in the region (January, February and December), with a maximum decrease of 325.25 kWh for January, whereas the energy demand for cooling had a maximum difference of 227.14 kWh. Moreover, the percentage deviation on the heating demand could be quite significant in the less cold months, since the deviation obtained was higher because the energy demand was lower, even achieving the full removal of the heating demand. Likewise, the energy demand for cooling presented a percentage deviation which oscillated around 3% in each of the months.

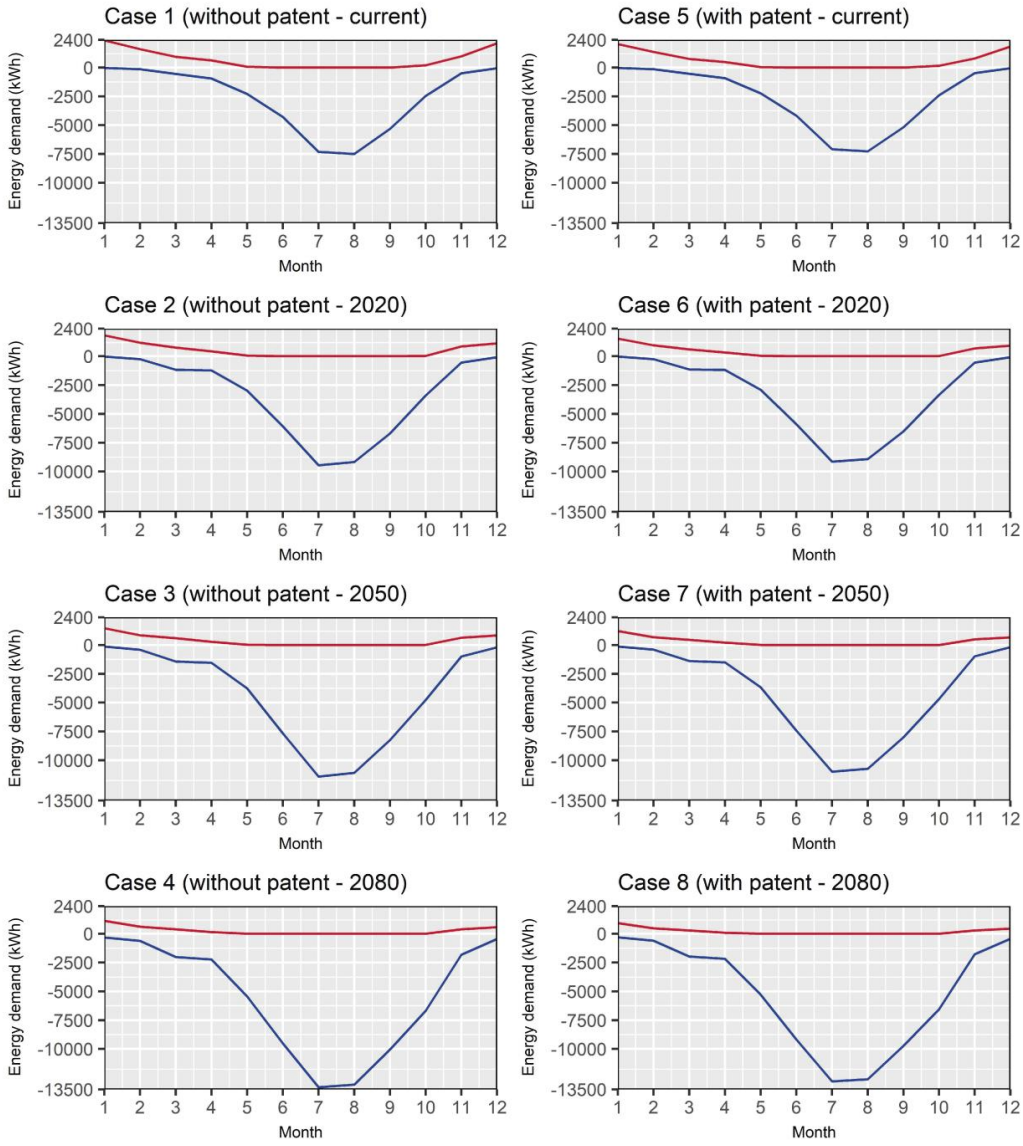

Figure 10. Monthly energy demand of the building for the different scenarios considered. The heating energy demand is represented by the red line, and the cooling energy demand by the blue line.

Table 5. Differential of energy demand between the case study without patent and the one with patent for the current period.

Month	Energy Demand for Heating			Energy Demand for Cooling		
	Without Patent (kWh)	With Patent (kWh)	Deviation	Without Patent (kWh)	With Patent (kWh)	Deviation
January	2358.80	2033.55	−13.79%	30.25	29.18	−3.54%
February	1605.04	1357.29	−15.44%	147.06	141.84	−3.55%
March	931.27	749.19	−19.55%	548.20	533.80	−2.63%
April	619.49	487.62	−21.29%	948.03	923.14	−2.63%
May	74.29	41.88	−43.62%	2285.62	2231.70	−2.36%
June	0.076	0.00	−100.00%	4291.06	4176.70	−2.67%
July	0.00	0.00	-	7316.86	7092.80	−3.06%
August	0.00	0.00	-	7501.44	7274.30	−3.03%
September	0.054	0.00	−97.67%	5317.10	5174.70	−2.68%
October	204.08	155.19	−23.96%	2464.60	2406.80	−2.34%
November	974.41	799.22	−17.98%	499.21	486.65	−2.52%
December	2111.37	1828.40	−13.40%	54.12	52.29	−3.39%

Table 6. Differential of energy demand between the case study without patent and the one with patent for the period of 2020.

Month	Energy Demand for Heating			Energy Demand for Cooling		
	Without Patent (kWh)	With Patent (kWh)	Deviation	Without Patent (kWh)	With Patent (kWh)	Deviation
January	1815.44	1529.57	−15.75%	24.46	23.57	−3.61%
February	1178.02	958.94	−18.60%	253.19	245.35	−3.10%
March	755.62	597.61	−20.91%	1170.50	1145.60	−2.13%
April	430.12	327.83	−23.78%	1216.95	1188.30	−2.36%
May	70.64	48.00	−32.05%	2983.77	2909.90	−2.48%
June	0.60	0.15	−75.10%	6076.84	5898.70	−2.93%
July	0.00	0.00	-	9458.50	9143.20	−3.33%
August	0.00	0.00	-	9178.80	8917.90	−2.84%
September	3.10	0.96	−68.95%	6693.96	6512.10	−2.72%
October	34.36	19.29	−43.87%	3400.38	3338.90	−1.81%
November	861.69	692.38	−19.65%	550.80	538.04	−2.32%
December	1130.68	923.19	−18.35%	84.87	81.80	−3.62%

Table 7. Differential of energy demand between the case study without patent and the one with patent for the period of 2050.

Month	Energy Demand for Heating			Energy Demand for Cooling		
	Without Patent (kWh)	With Patent (kWh)	Deviation	Without Patent (kWh)	With Patent (kWh)	Deviation
January	1462.32	1221.28	−16.48%	126.04	121.69	−3.45%
February	854.57	679.25	−20.52%	406.84	396.93	−2.44%
March	588.29	458.80	−22.01%	1422.66	1393.00	−2.08%
April	283.27	210.83	−25.58%	1537.58	1500.40	−2.42%
May	28.98	20.80	−28.24%	3766.21	3668.40	−2.60%
June	0.00	0.00	−100.00%	7664.74	7422.00	−3.17%
July	0.00	0.00	-	11,410.26	10,996.00	−3.63%
August	0.00	0.00	-	11,092.09	10,741.00	−3.17%
September	0.21	0.00	−99.04%	8245.97	8008.70	−2.88%
October	9.04	4.15	−54.11%	4772.79	4683.50	−1.87%
November	634.55	500.38	−21.14%	995.39	973.23	−2.23%
December	829.98	667.73	−19.55%	192.27	186.18	−3.17%

Table 8. Differential of energy demand between the case study without patent and the one with patent for the period of 2080.

Month	Energy Demand for Heating			Energy Demand for Cooling		
	Without Patent (kWh)	With Patent (kWh)	Deviation	Without Patent (kWh)	With Patent (kWh)	Deviation
January	1127.26	929.58	−17.54%	313.54	303.67	−3.15%
February	613.16	472.73	−22.90%	616.55	603.16	−2.17%
March	387.42	293.10	−24.35%	2014.46	1972.20	−2.10%
April	141.69	98.39	−30.56%	2226.95	2170.40	−2.54%
May	5.67	4.11	−27.48%	5440.69	5284.60	−2.87%
June	0.00	0.00	-	9509.69	9168.50	−3.59%
July	0.00	0.00	-	13,318.91	12,805.00	−3.86%
August	0.00	0.00	-	13,093.10	12,631.00	−3.53%
September	0.00	0.00	-	10,049.26	9728.40	−3.19%
October	0.58	0.16	−72.68%	6689.45	6560.10	−1.93%
November	390.52	296.36	−24.11%	1811.96	1774.20	−2.08%
December	575.59	452.65	−21.36%	448.87	437.20	−2.60%

Regarding the future scenarios, the effect generated by the patented building solution on the heating demand was decreasing, with values of monthly maximum differential of 285.87 kWh for 2020, 241.04 kWh for 2050, and 197.68 kWh for 2080. This was due to the decrease of heating demand caused by the increase of the external temperatures. However, the use of the building patent in the

simulation allowed reductions up to 21.36% for the coldest months, so although its influence is lower in future scenarios, the energy demand for heating is being reduced considerably. On the other hand, the maximum decrease in cooling demand that generated the improvement of the thermal bridge allowed one to achieve monthly maximum reductions of 315.33 kWh for 2020, 414.72 kWh for 2050, and 513.77 kWh for 2080.

Therefore, the effect of the patent for improving the thermal bridge of the slab front on the global energy demand of the building was quite significant. Figure 11 represents the global energy demands for heating and cooling, as well as the total demand for each assumption studied. As it can be seen, the decrease obtained in the heating demand was very significant, even in future scenarios characterized by less heating demand. In this sense, the decrease achieved by year was of 18.83% in 2020, 19.78% in 2050, and 21.43% in 2080. On the other hand, the global decrease in cooling demand had the same rate of percentage decrease for all the scenarios considered, varying between 2.80% for the current scenario and 3.20% for the scenario in 2080. Thus, the improvement of the thermal bridge of the slab front allowed to reduce the energy demand of the building in the different scenarios considered, with a saving on the heating energy demand higher than 18%, and on the cooling energy demand higher than 2.80%.

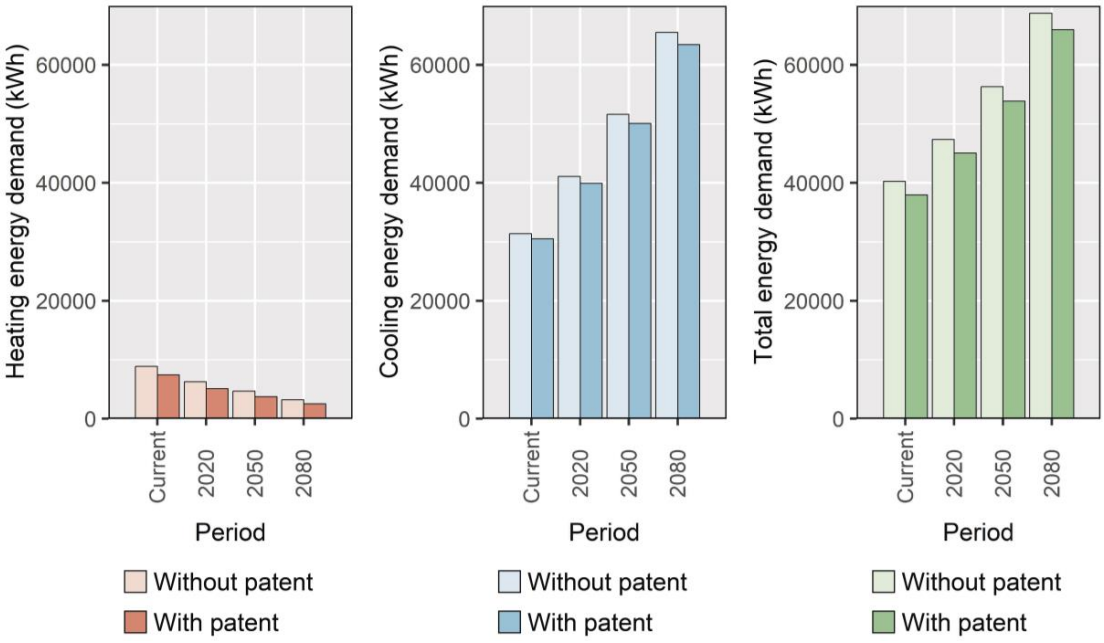

Figure 11. Global energy demand of the building for the different scenarios considered.

5. Conclusions

This article studies the effect of the thermal bridge of slab front on the energy demand of a building. Firstly, five patented construction solutions for thermal bridges in slab fronts in a certain case study were analysed by means of two-dimensional simulation, determining the best patent solution for the building. Then, energy simulations of the case study in different time scenarios (current, 2020, 2050 and 2080) were carried out by analysing the effect of improving the thermal bridge in the slab front on the energy demand of the building. Based on the results obtained, the following conclusions can be drawn:

- From the five patents analysed, the one which obtained the lowest linear thermal transmittance (ψ) was Patent 5, with a reduction of 95.74% with respect to the linear thermal transmittance that the slab front of the analysed building presents. The rest of the patents obtained lower decreases, and even a higher linear thermal transmittance was obtained by Patent 4.

- The temperature factor for the interior surface ($f_{R,si}$) for both constructive solution of the case study and the different patents analysed exceeded the value required by the estate rules which guaranteed that condensations were not generated. Thus, the climate conditions typical of the analysis region (Csa classification according to Köppen-Geiger) allowed to guarantee a low condensation risk due to the thermal bridges of the slab fronts.
- The improvement of the thermal bridge in the slab front allowed to achieve important decreases on the heating demand in the current scenario, with differences up to 325.25 kWh during the month of the highest demand. Regarding the cooling energy demand, the change generated by the improvement of the thermal bridge was lower, although reductions by 227.14 kWh were obtained in the summer months.
- For future scenarios, the effect generated by the increase of the outdoor temperatures with a lower heating demand and a higher cooling demand affected the incidence of the improvement of the thermal bridge on the energy behaviour of the building. In this sense, the monthly reduction of the heating energy demand generated by the improvement of the thermal bridge presented a decreasing behaviour, with the following values of maximum decrease: 285.87 kWh (2020), 241.04 kWh (2050), and 197.68 (2080). Despite of this, the percentage decrease on the global energy demand for heating had a growing behaviour, with deviations of 18.83% (2020), 19.78% (2050), and 21.43% (2080).

On the other hand, the cooling demand presented a growing tendency in the monthly maximum decreases in the different scenarios analysed, with maximum decreases of 315.33 kWh in 2020, 414.72 kWh in 2050, and 513.77 kWh in 2080.

Therefore, the improvement of the thermal bridge of the slab front by using the best patent analysed led to global reductions on the energy demand for heating higher than 18%, whereas on the energy demand for cooling were higher than 2.80% in all the time scenarios considered.

To conclude, it is important to highlight that there are no studies where the thermal behaviour of different patented designs for thermal bridges in slab fronts is studied, as well as the effect that these solutions havee on the energy demand of the building, both in current and future scenarios. In this sense, despite the progressive reduction of heating demand and the increase of cooling demand, the improvement of the thermal bridge of the slab front allows one to reduce significantly the energy demand of the building. Thus, this is an aspect that should be considered in both design phase and energy audits of the existing buildings, with the aim of guaranteeing an adequate energy behaviour of the building.

Author Contributions: All authors took part in the choice of the case studies, performed the measurement, managed and analysed data, and wrote the document.

Funding: This research received no external funding.

Acknowledgments: The authors would like to acknowledge the VI Own Research Plan University of Seville for their support in this research.

Conflicts of Interest: The authors declare no conflict of interest.

References

1. European Environment Agency. Final Energy Consuption by Sector and Fuel. Available online: https://www.eea.europa.eu/data-and-maps/indicators/final-energy-consumption-by-sector-9/assessment-1 (accessed on 19 August 2018).
2. European Academy of Bolzano. *European Project iNSPiRe Report*; European Academy of Bolzano: Bolzano, Italy, 2015.
3. European Commission. *A Roadmap for Moving to A Competitive Low Carbon Economy in 2050*; European Commission: Brussels, Belgium, 2011; pp. 1–15.
4. Rubio-Bellido, C.; Pérez-Fargallo, A.; Pulido-Arcas, J.A. Optimization of annual energy demand in office buildings under the influence of climate change in Chile. *Energy* **2016**, *114*, 569–585. [CrossRef]

5. Sánchez-García, D.; Rubio-Bellido, C.; Marrero Meléndez, M.; Guevara-García, F.J.; Canivell, J. El control adaptativo en instalaciones existentes y su potencial en el contexto del cambio climático. *Hábitat Sustentable* **2017**, *7*, 6–17. [CrossRef]
6. Battista, G.; Evangelisti, L.; Guattari, C.; Basilicata, C.; de Lieto Vollaro, R. Buildings Energy Efficiency: Interventions Analysis under a Smart Cities Approach. *Sustainability* **2014**, *6*, 4694–4705. [CrossRef]
7. Mortarotti, G.; Morganti, M.; Cecere, C. Thermal analysis and energy-efficient solutions to preserve listed building façades: The INA-Casa building heritage. *Buildings* **2017**, *7*, 1–22. [CrossRef]
8. Park, K.; Kim, M. Energy Demand Reduction in the Residential Building Sector: A Case Study of Korea. *Energies* **2017**, *10*, 1–11. [CrossRef]
9. Goggins, J.; Moran, P.; Armstrong, A.; Hajdukiewicz, M. Lifecycle environmental and economic performance of nearly zero energy buildings (NZEB) in Ireland. *Energy Build.* **2016**, *116*, 622–637. [CrossRef]
10. International Organization for Standardization. *ISO 10211:2017-Thermal Bridges in Building Construction-Heat Flows and Surface Temperatures-Detailed Calculations*; International Organization for Standardization: Geneva, Switzerland, 2017.
11. Balaras, C.A.; Argiriou, A.A. Infrared thermography for building diagnostics. *Energy Build.* **2002**, *34*, 171–183. [CrossRef]
12. Sajjadian, S. Risk Identification in the Early Design Stage Using Thermal Simulations—A Case Study. *Sustainability* **2018**, *10*, 262. [CrossRef]
13. Capozzoli, A.; Gorrino, A.; Corrado, V. A building thermal bridges sensitivity analysis. *Appl. Energy* **2013**, *107*, 229–243. [CrossRef]
14. Šadauskiene, J.; Ramanauskas, J.; Šeduikyte, L.; Daukšys, M.; Vasylius, A. A simplified methodology for evaluating the impact of point thermal bridges on the high-energy performance of a Passive House. *Sustainability* **2015**, *7*, 16687–16702. [CrossRef]
15. Aguilar, F.; Solano, J.P.; Vicente, P.G. Transient modeling of high-inertial thermal bridges in buildings using the equivalent thermal wall method. *Appl. Therm. Eng.* **2014**, *67*, 370–377. [CrossRef]
16. Martin, K.; Erkoreka, A.; Flores, I.; Odriozola, M.; Sala, J.M. Problems in the calculation of thermal bridges in dynamic conditions. *Energy Build.* **2011**, *43*, 529–535. [CrossRef]
17. Fantucci, S.; Isaia, F.; Serra, V.; Dutto, M. Insulating coat to prevent mold growth in thermal bridges. *Energy Procedia* **2017**, *134*, 414–422. [CrossRef]
18. Brás, A.; Gonçalves, F.; Faustino, P. Cork-based mortars for thermal bridges correction in a dwelling: Thermal performance and cost evaluation. *Energy Build.* **2014**, *72*, 296–308. [CrossRef]
19. Echarri, V. Thermal ceramic panels and passive systems in mediterranean housing: Energy savings and environmental impacts. *Sustainability* **2017**, *9*. [CrossRef]
20. Ascione, F.; Bianco, N.; De Rossi, F.; Turni, G.; Vanoli, G.P. Different methods for the modelling of thermal bridges into energy simulation programs: Comparisons of accuracy for flat heterogeneous roofs in Italian climates. *Appl. Energy* **2012**, *97*, 405–418. [CrossRef]
21. Asdrubali, F.; Baldinelli, G.; Bianchi, F. A quantitative methodology to evaluate thermal bridges in buildings. *Appl. Energy* **2012**, *97*, 365–373. [CrossRef]
22. Asdrubali, F.; Baldinelli, G.; Bianchi, F.; Costarelli, D.; Rotili, A.; Seracini, M.; Vinti, G. Detection of thermal bridges from thermographic images by means of image processing approximation algorithms. *Appl. Math. Comput.* **2018**, *317*, 160–171. [CrossRef]
23. Bianchi, F.; Pisello, A.L.; Baldinelli, G.; Asdrubali, F. Infrared thermography assessment of thermal bridges in building envelope: Experimental validation in a test room setup. *Sustainability* **2014**, *6*, 7107–7120. [CrossRef]
24. Garrido, I.; Lagüela, S.; Arias, P.; Balado, J. Thermal-based analysis for the automatic detection and characterization of thermal bridges in buildings. *Energy Build.* **2018**, *158*, 1358–1367. [CrossRef]
25. O'Grady, M.; Lechowska, A.A.; Harte, A.M. Infrared thermography technique as an in-situ method of assessing the heat loss through thermal bridging. *Energy Build.* **2017**, *135*, 20–32. [CrossRef]
26. O'Grady, M.; Lechowska, A.A.; Harte, A.M. Quantification of heat losses through building envelope thermal bridges influenced by wind velocity using the outdoor infrared thermography technique. *Appl. Energy* **2017**, *208*, 1038–1052. [CrossRef]
27. Zalewski, L.; Lassue, S.; Rousse, D.; Boukhalfa, K. Experimental and numerical characterization of thermal bridges in prefabricated building walls. *Energy Convers. Manag.* **2010**, *51*, 2869–2877. [CrossRef]

28. Tadeu, A.; Simões, I.; Simões, N.; Prata, J. Simulation of dynamic linear thermal bridges using a boundary element method model in the frequency domain. *Energy Build.* **2011**, *43*, 3685–3695. [CrossRef]
29. Dilmac, S.; Guner, A.; Senkal, F.; Kartal, S. Simple method for calculation of heat loss through floor/beam-wall intersections according to ISO 9164. *Energy Convers. Manag.* **2007**, *48*, 826–835. [CrossRef]
30. Theodosiou, T.G.; Papadopoulos, A.M. The impact of thermal bridges on the energy demand of buildings with double brick wall constructions. *Energy Build.* **2008**, *40*, 2083–2089. [CrossRef]
31. Theodosiou, T.; Tsikaloudaki, K.; Bikas, D. Analysis of the Thermal Bridging Effect on Ventilated Facades. *Proced. Environ. Sci.* **2017**, *38*, 397–404. [CrossRef]
32. Ramalho de Freitas, J.; Grala da Cunha, E. Thermal bridges modeling in South Brazil climate: Three different approaches. *Energy Build.* **2018**, *169*, 271–282. [CrossRef]
33. Ge, H.; McClung, V.R.; Zhang, S. Impact of balcony thermal bridges on the overall thermal performance of multi-unit residential buildings: A case study. *Energy Build.* **2013**, *60*, 163–173. [CrossRef]
34. Zedan, M.F.; Al-Sanea, S.; Al-Mujahid, A.; Al-Suhaibani, Z. Effect of Thermal Bridges in Insulated Walls on Air-Conditioning Loads Using Whole Building Energy Analysis. *Sustainability* **2016**, *8*, 1–20. [CrossRef]
35. Song, J.H.; Lim, J.H.; Song, S.Y. Evaluation of alternatives for reducing thermal bridges in metal panel curtain wall systems. *Energy Build.* **2016**, *127*, 138–158. [CrossRef]
36. Evola, G.; Margani, G.; Marletta, L. Energy and cost evaluation of thermal bridge correction in Mediterranean climate. *Energy Build.* **2011**, *43*, 2385–2393. [CrossRef]
37. Santos, P.; Martins, C.; Da Silva, L.S.; Bragança, L. Thermal performance of lightweight steel framed wall: The importance of flanking thermal losses. *J. Build. Phys.* **2014**, *38*, 81–98. [CrossRef]
38. Martins, C.; Santos, P.; Da Silva, L.S. Lightweight steel-framed thermal bridges mitigation strategies: A parametric study. *J. Build. Phys.* **2016**, *39*, 342–372. [CrossRef]
39. Roque, E.; Santos, P. The Effectiveness of Thermal Insulation in Lightweight Steel-Framed Walls with Respect to Its Position. *Buildings* **2017**, *7*, 13. [CrossRef]
40. Levinskyte, A.; Banionis, K.; Geleziunas, V. The Influence of Thermal Bridges for Buildings Energy -Consumption of "A" Energy Efficiency Class. *J. Sustain. Archit. Civ. Eng.* **2016**, *15*, 47–58. [CrossRef]
41. Société Générale d'Entreprises Construction. Method for the Construction and Insulation of a Building Having a Masonry-Lined Facade Fastened to an Intermediate Floor. Patent FR2542347B1, 14 September 1984. Available online: https://patents.google.com/patent/FR2542347B1/en (accessed on 19 August 2018).
42. Egger, W. Shuttering Element. Patent DE3542651A1, 21 February 1985. Available online: https://patents.google.com/patent/DE3542651A1/en (accessed on 19 August 2018).
43. François, M. Thermal Flow Breaker for Wall and Floor Slab Joint Comprises Thin Insulating Element Folded along Pre-Marked Lines to Cover Floor Slab Edge. Patent FR2839994A1, 28 November 2003. Available online: https://patents.google.com/patent/FR2839994A1/en (accessed on 19 August 2018).
44. López Muñoz, R. Recubrimiento para Cantos de Forjado. Patent ES2387165A1, 17 September 2012. Available online: https://patents.google.com/patent/ES2387165A1/en (accessed on 19 August 2018).
45. Ortega López, H.; Moyano Campos, J.J.; Marín García, D.; Rico Delgado, F.; Moreno Muñoz, A. Sistema Estructural Contra el Puente Térmico en Frente de Forjados para Fachadas Cerámicas. Patent ES2537251B1, 30 April 2015. Available online: https://patents.google.com/patent/ES2537251B1/ar (accessed on 19 August 2018).
46. Ficco, G.; Iannetta, F.; Ianniello, E.; D'Ambrosio Alfano, F.R.; Dell'Isola, M. U-value in situ measurement for energy diagnosis of existing buildings. *Energy Build.* **2015**, *104*, 108–121. [CrossRef]
47. International Organization for Standardization. *ISO 6781:1983-Thermal Insulation-Qualitative Detection of Thermal Irregularities in Building Envelopes-Infrared Method*; International Organization for Standardization: Geneva, Switzerland, 1983.
48. International Organization for Standardization (ISO). *British Standards Building Components and Building Elements-Thermal Resistance and Thermal Transmittance-Calculation Method*; International Organization for Standardization: Geneva, Switzerland, 2007.
49. Rubel, F.; Kottek, M. Observed and projected climate shifts 1901–2100 depicted by world maps of the Köppen-Geiger climate classification. *Meteorol. Z.* **2010**, *19*, 135–141. [CrossRef]
50. Hilderson, W. Therm 7.4 Validation According to EN ISO 10211: 2007. 2016. Available online: https://pixii.be/sites/default/files/therm_7.4_validatie_10211.pdf (accessed on 19 August 2018).

51. Nammi, S.K.; Shirvani, H.; Shirvani, A.; Edwards, G.; Whitty, J.P.M. *Verification of Calculation Code THERM in Accordance with BS EN ISO 10077-2*; Anglia Ruskin University: Chelmsford, UK, 2014; ISBN 9780956560889.
52. Belcher, S.; Hacker, J.; Powell, D. Constructing design weather data for future climates. *Build. Serv. Eng. Res. Technol.* **2005**, *26*, 49–61. [CrossRef]
53. Jentsch, M.F.; Bahaj, A.B.S.; James, P.A.B. Climate change future proofing of buildings-Generation and assessment of building simulation weather files. *Energy Build.* **2008**, *40*, 2148–2168. [CrossRef]
54. Jentsch, M.F.; James, P.A.B.; Bourikas, L.; Bahaj, A.B.S. Transforming existing weather data for worldwide locations to enable energy and building performance simulation under future climates. *Renew. Energy* **2013**, *55*, 514–524. [CrossRef]
55. Nakicenovic, N.; Swart, R. *Special Report on Emissions Scenarios. A Special Report of Working Group III of the Intergovernmental Panel on Climate Change*; Cambridge University Press: Cambridge, UK, 2000; ISBN 0-521-80493-0.
56. Spanish Ministry of Public Service. *Spanish Technical Building Code-Royal Decree 314/2006, 17th of March 2006*; Spanish Ministry of Public Service: Madrid, Spain, 2013.
57. ASHRAE. *Handbook of Fundamentals*; The American Society of Heating Refrigerating and Air-Conditioning Engineers: Atlanta, GA, USA, 2013; ISBN 9781936504466.